NONE

Security Classification

DOCUMENT CONTROL DATA - R & D

(Security classification of title, body of abstract and indexing annotation must be entered when the overall report is classified)

1. ORIGINATING ACTIVITY *(Corporate author)* Massachusetts Institute of Technology	2a. REPORT SECURITY CLASSIFICATION 2b. GROUP

3. REPORT TITLE

oBSERVATIONS OF THE MEAN WIND PROFILE OVER THE OPEN OCEAN

4. DESCRIPTIVE NOTES *(Type of report and inclusive dates)*

Technical Report from June 1961 thesis

5. AUTHOR(S) *(First name, middle initial, last name)*

William D. Groscup, CDR U.S. Navy

6. REPORT DATE November 1971	7a. TOTAL NO. OF PAGES 49	7b. NO. OF REFS 7
8a. CONTRACT OR GRANT NO. N00014-67-A-0204-0024 b. PROJECT NO. NR 083-236 c. d.	9a. ORIGINATOR'S REPORT NUMBER(S) 71-7 9b. OTHER REPORT NO(S) *(Any other numbers that may be assigned this report)*	

10. DISTRIBUTION STATEMENT

Distribution of this document is unlimited.

11. SUPPLEMENTARY NOTES	12. SPONSORING MILITARY ACTIVITY Office of Naval Research Washington, D.C. 20360

13. ABSTRACT

The purpose of this study was to investigate the mean wind speed profile over the open ocean.

Analysis of wind profile data showed that averaging periods must be considered when the profile form is discussed since 95 percent of the 10 minute averaged profiles were found to be logarithmic while less than 50 percent of the 10 second averaged profiles were logarithmic. This analysis also showed that the roughness length z_o, was highly structured with singularities at 2, 4, 8 and 12 meters/sec. The friction veloctiy is shown to possess a bi-modal form at these wind speeds and appears to bear a linear relationship to the ten meter wind speed within the intervals between the singularities in z_o.

The turbulent energy production term as determined from profile parameters was investigated and found to vary by 3 orders of magnitude over time intervals of the same order as those of surface wave periods.

DD FORM 1 NOV 65 1473 (PAGE 1)

S/N 0102-014-6600

NONE

Security Classification

NONE

Security Classification

14 KEY WORDS	LINK A		LINK B		LINK C	
	ROLE	WT	ROLE	WT	ROLE	WT
Boundary Layer						
Sea-Surface Boundary Layer						
Turbulence						
Wind Stress						
Roughness Length						
Intermittency						
Turbulent Production						
Air-Sea Interaction						

NONE

Security Classification

Report No. 71-7

OBSERVATIONS OF THE MEAN WIND PROFILE OVER THE OPEN OCEAN

by

William Dale Groscup

M.S. Thesis

Massachusetts Institute of Technology

Department of Meteorology

November 1971

Report 71-7

Work Sponsored by

Office of Naval Research under

Contract No. N00014-67-A-0204-0024

Contract Authority NR 083-236

Observations of the Mean Wind Profile over the Open Ocean

William Dale Groscup

Abstract

The purpose of this study was to investigate the mean wind speed profile over the open ocean.

Analysis of wind profile data showed that averaging periods must be considered when the profile form is discussed since 95 percent of the 10 minute averaged profiles were found to be logarithmic while less than 50 percent of the 10 second averaged profiles were logarithmic. This analysis also showed that the roughness length, z_o, was highly structured with singularities at 2, 4, 8 and 12 meters/sec. The friction velocity is shown to possess a bi-modal form at these wind speeds and appears to bear a linear relationship to the ten meter wind speed within the intervals between the singularities in z_o.

The turbulent energy production term as determined from profile parameters was investigated and found to vary by 3 orders of magnitude over time intervals of the same order as those of surface wave periods.

Thesis Supervisor: Erik L. Mollo-Christensen

Title: Professor of Meteorology

Table of Contents

Tables

List of Illustrations

I. Introduction

Although man has observed the existence of a relationship between wind and waves for many centuries, only in the twentieth century has he expended any appreciable scientific effort in an attempt to explain the generation of surface water waves by wind. The non-linearity of the equations involved and the turbulence of the wind field, which defies reproduction, cause both mathematical and laboratory models to fail in their explanation of the details of wave growth. Models representing the extremely large Reynolds numbers of a typical oceanic wind field are impossible to design, thus the intermittent nature of turbulence associated with high Reynolds numbers is usually neglected. Only average values of the wind field, which are reproducible, are considered by most investigators.

That the oceanic wind field is truely intermittent has been clearly confirmed by Van Atta and Chen (1970). Their data was obtained aboard R/V FLIP during the Barbados Oceanographic and Meteorological Experiment (BOMEX). The advent of stable open-ocean instrument platforms such as the R/V FLIP, belonging to the Scripps Institute of Oceanography, the "Trition" of the Florida State University (Warsh et al [1970]) and the air-sea interaction buoy of the Massachusetts Institute of Technology (Mollo-Christensen and Dorman [1971]) have made investigations of the oceanic boundary layer possible.

By use of the telemetered signals from the M.I.T. buoy, wind speed profiles and wave height data have been recorded remotely for a wide range of wind speeds. This report is an attempt to refine and to verify

the wind profile analysis conducted by Ruggles (1969) and to consider effects of the intermittent nature of the wind field and its effects on the wind profile.

II. Field Facilities and Instrumentation

II.1 Site

The site selected for the M.I.T. air-sea interaction field investigation during the summer and fall of 1970 was at the entrance of Vineyard Sound. Figure 1, a chart of the local area, shows both local geography and the site of the field investigation. The site's proximity to the islands of Martha's Vineyard, 4.1 nautical miles to the east, and the Elizabeth Island chain to the northeast and north provided a degree of protection from strong northerly winds and concomitant high sea states of early winter storms. This lee enabled the observation program to extend into December with minimal damage to instruments and buoy while still providing an open fetch of deep water for wind and wave directions between 150° and 270°. Water depth at the site was 31 meters, gradually increasing with distance in these southerly directions.

Orientation of the moored instrument platform was found to depend upon the direction of the strong tidal current and to be independent of wind direction for all observed wind velocities. Average maximum speed of the tidal current at the site was 1.1 meters/second.

Prevailing wind and wave direction in this area during the summer and early fall is south-southwest. Typical wind conditions encountered during the observational program were light southerly winds during the early morning hours increasing during the afternoon to south - southwesterly 4 to 10 meters/second (due to the sea-breeze effect) and then decreasing during the late afternoon and early evening hours to southerly 2 to 4 meters/second.

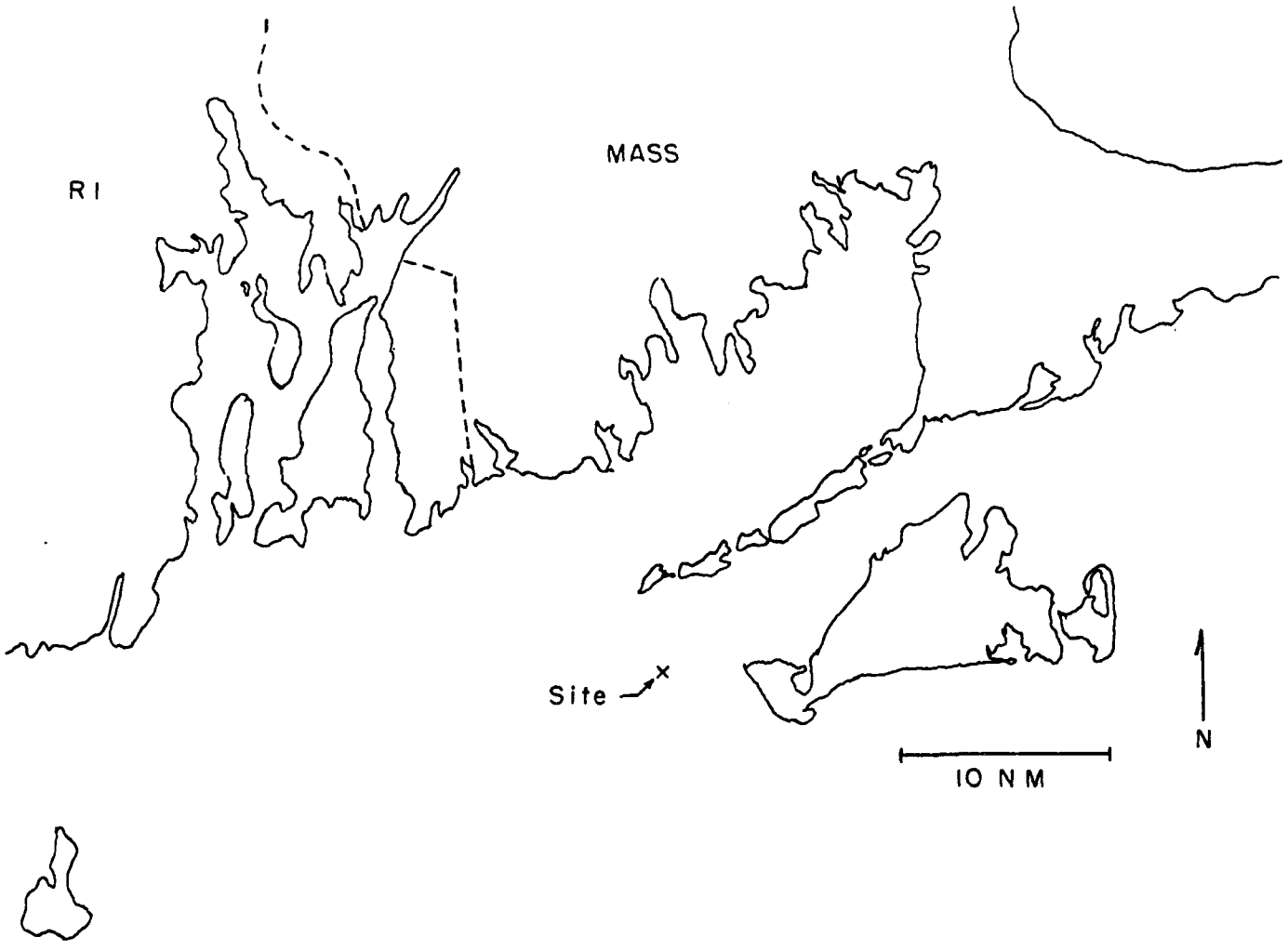

Figure 1: Site for air-sea interaction investigation.

Thus the site selected provided an unlimited fetch of deep water to the south, a large range of wind speeds, and a predictable buoy orientation based on the known tidal ellipse.

II.2 Instrument Platform

A tubular spar buoy designed by Professor Mollo-Christensen and built by Dan Clark Incorporated was used as the instrument platform for the 1970 field investigation. This buoy is shown in Figure 2. Its overall length is 112 feet with 41 feet extending above the mean water level. The compartmentalized buoy's lower chamber floods completely when the buoy is erect. The upper compartment contains compressed air capable of purging the lower compartment of its water ballast to return the buoy to the horizontal position for towing to a new site. A 50 foot section of triangular radio tower is attached to the main buoy eight feet from the tubular sections to serve as a track for subsurface and near surface instruments. A mast, consisting of a 30 feet section of a triangular radio tower, extended vertically above the small working platform. The entire system had a damped resonance frequency of .07 Hz.

Once the buoy was moored at the selected site and raised to the vertical by ballasting, permanent electronics and instruments were installed. This equipment consisted of a 12 volt, nickel-cadmium battery purchased from the Advanced Technology and Systems Corporation. This battery, rated at 120 ampere-hours, was capable of operating the instruments and telemetry system for 12 hours without recharging. The battery and the telemetry electronics were installed in a 5 foot deep compartment built into the uppermost portion of the main buoy. Ready access was

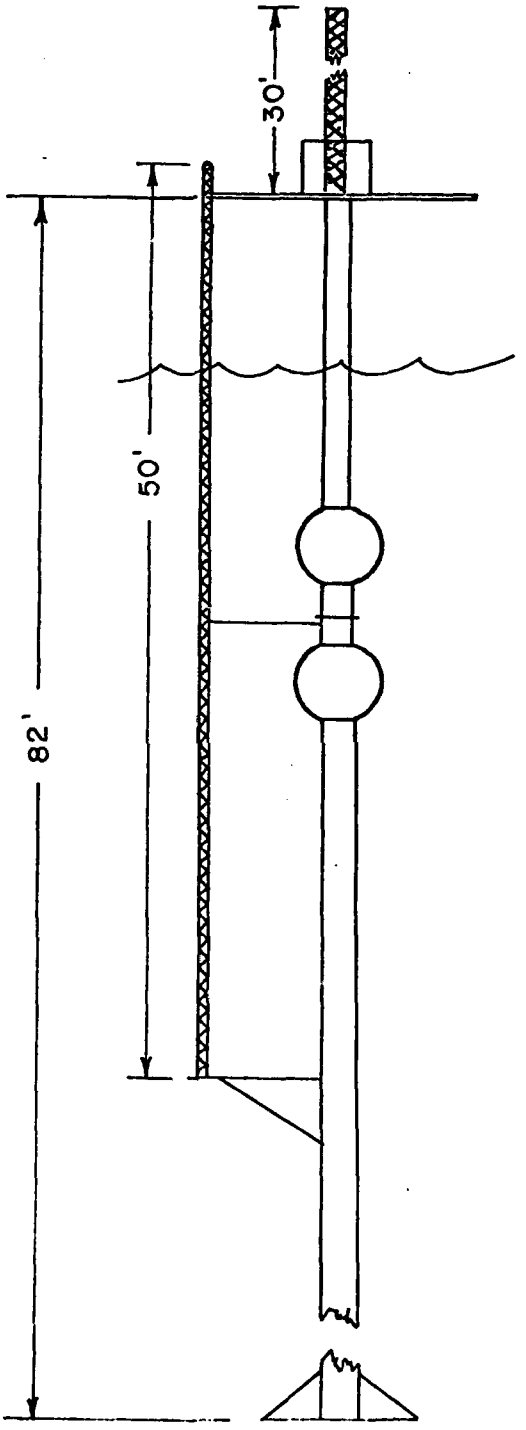

Figure 2: Instrument platform design.

available to the electronics through a bulkhead located on the working platform. A continuous charge was provided to the battery through a thermoelectric generator model 515-12 manufactured by the Minnesota Mining and Manufacturing Company. The generator, mounted adjacent to the working platform, was capable of producing 30 ampere-hours per day while burning approximately 1/2 pound of propane gas.

Permanently installed instruments consisted of one wave gauge and five cup-anamometers attached to the buoy at 2.4, 3.7, 5.0, 7.5 and 11.4 meters above the mean water level. The five anemometers were connected to a single data channel via a ring counter sampling circuit. Approximately 100 hours of wind speed profile and wave gauge data were recorded using these instruments.

II.3 Shore Facilities

A large decommissioned boathouse and pier belonging to the U.S. Coast Guard on Cuttyhunk Island, Massachusetts, was obtained for the project. The pier provided ample docking space for all floating stock used during the investigation, while the boathouse provided storage and working spaces, in addition to a ground station for the data acquisition system. A small weather station was also maintained in and adjacent to the boathouse.

II.4 Boats and small craft

The M.I.T. oceanographic research boat, the R/V R.R. Shrock was used for transportation of personnel and equipment to and from the field

site. A 12 foot Zodiak rubber boat was towed by the R/V R.R. Shrock and used for transfers of men and equipment between the instrument platform and the R/V R.R. Shrock. The R/V R.R. Shrock also provided backup voice communication system between the buoy and the ground station on Cuttyhunk Island via citizens band radio.

II.5 Data Acquisition

During the summer of 1969 wind speed and wave height profiles were recorded to test a new telemetered data acquisition system. This system had been part of an Atlas Missile Telemetry System declared excess equipment by the U.S. Air Force. A block diagram of the system as it had been modified for use during the summer of 1970 is shown in Figure 3. An instrument senses a physical variable; its conditioned output is used to drive a voltage controlled oscillator, which in turn is mixed with the other signals prior to transmission. The frequency modulated signal is then transmitted to the receiving station (ground station) on Cuttyhunk Island approximately 4 nautical miles to the north. The signal was recorded on a Hewlett-Packard model 3960 tape recorder with 30 minute recording capacity and a 60 KHz bandwidth. Signals may then be separated using the discriminator system. This system of data acquisition proved to be extremely reliable.

There were 12 channels of information available for use by the investigator. These channels were made completely interchangeable by changing the sensing probe and conditioning amplifier of an individual channel.

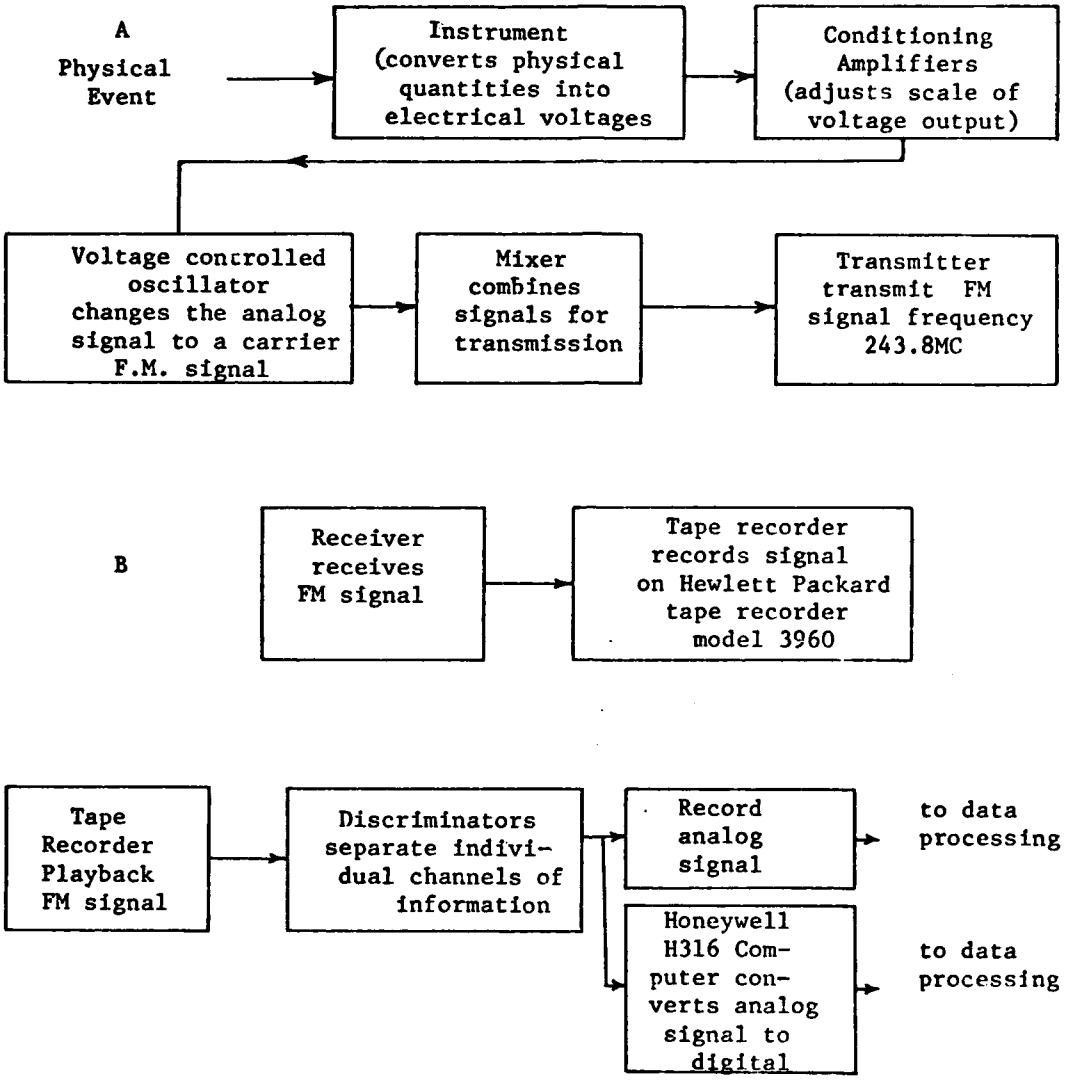

Figure 3: Block diagram of data acquisition system.

In addition to the transmission of data representing physical processes of the ocean and the atmosphere, a standard 25 KHz frequency was also transmitted for synchronization and compensation of the signals during the recording and subsequent playback of the data.

II.6 Instrumentation

Cup Anemometers: Six anemometers were rebuilt at M.I.T. for use by the project during the investigations of 1969 and 1970. A 3-cup design was employed. Their principle of operation involved the interruption of a light beam by a chopping wheel attached to the cup axes. The light was sensed by a photoresistor, which, by the use of appropriate circuitry, produced square output pulses. The counting of these pulses gave the measured wind speed, since the calibration of each instrument was known. Cup anemometer calibrations were performed in the MIT low-turbulence wind tunnel. A distance constant of 101 cm/count was obtained. The analog output of the cup anemometers was linear over the range of speeds used during calibration (0 to 25 meters/second).

Hot-film Anemometers: Based upon the recommendation of Ruggles (1969), six Disa S & B battery operated constant temperature, hot-film anemometers were used to investigate small scale features of the maritime atmosphere. A total of 18 Disa 55A81 pyrex-backed hot-film probes were purchased and calibrated. An overheat ratio of 1.55:1 was used to safeguard probe life and still yield the dynamic response required during the investigation.

The probes were calibrated in the MIT low-turbulence wind tunnel over a range of wind speeds from 0 to 15 meters/second.After careful attention to grounding and sealing problems, as well as procedures for operation and mounting, the probes performed well in the field and are highly recommendable for future use. It should be emphasized, however, that these probes are delicate instruments and should be handled accordingly.

Wave Gauge: Four capacitance-type wave gauges were built at MIT to measure water level. The sensors consisted of standard outboard motor steering cable. The stainless steel wire core and the sea water served as positive and negative plates while the plastic coating of the wire served as the dielectric. The capacitance of the cable, which is proportional to the depth of immersion, controlled an oscillator whose frequency was beat against another oscillator set at 30.1 KHz. The resulting frequency varied between 300 and 700 Hz depending on wave height.

Both 15 foot and 5 foot sensor lengths were used. A one centimeter change in water height was equivalent to a frequency charge of 1.4 Hz when using the 15 foot sensor and 3.2 Hz when using the 5 foot sensor. All wave gauges performed well all summer.

III. Vertical Mean Wind Profile Measurements Over the Open Ocean

During the summers of 1969 and 1970, a total of 1493 minutes of wind and wave data was recorded in conjunction with the MIT air-sea interaction investigation in Vineyard Sound. The high reliability of cup anemometers and a remotely controlled telemetry system permitted data acquisition over a wide range of wind speeds. Data were recorded on a Hewlett-Packard tape recorder (model 3960) located in the boathouse at Cuttyhunk Island. Tapes were then returned to MIT where they were processed both by analog and digital methods.

Since Ruggles (1969) had shown by his analysis of mean wind profiles, that over 96% of his wind profiles could be considered logarithmic, a "least squares" logarithmic curve-fitting program was developed for use on the Honeywell H 316 computer. By assuming the wind profile to be linear in log Z and applying the method of least squares a curve fitting program was developed as follows: Given the equation for the desired straight line $U = a_0 + a_1 \ln Z$;

where U is the velocity, a_0 & a_1, are constants and $\ln Z$ is the natural logarithm of height, then values of velocity on the line corresponding to heights $\ln Z_i$ are $a_0 + a_1 \ln Z_i$, while actual values of velocity are U_i where $i = 1, 2, 3, \ldots n$. The least squares principle requires that the sum of the squares of the difference, ϵ, between these two velocity values be a minimum. Thus a straight line is desired such that $\sum_{i=1}^{n} \epsilon_i^2 = (a_0 + a_1 \ln Z_1 - U_1)^2 + \ldots + (a_0 + a_1 \ln Z_n - U_n)^2$

is a minimum or

$$n a_0 + a_1 \Sigma \ln z_i - \Sigma U = 0$$

$$a_0 \Sigma \ln z + a_1 \Sigma (\ln z)^2 - \Sigma U \Sigma \ln z = 0 \qquad \text{where } \Sigma = \sum_{i=1}^{n}$$

solving for a_0 and a_1 yields

$$a_0 = \frac{\Sigma U \Sigma (\ln z)^2 - \Sigma \ln z \Sigma U \Sigma \ln z}{n \Sigma (\ln z)^2 - (\Sigma \ln z)^2}$$

$$a_1 = \frac{n \Sigma U (\ln z) - \Sigma U \Sigma \ln z}{n \Sigma (\ln z)^2 - (\Sigma \ln z)^2}$$

a_1 is the slope of the line and is related to a measure of the "goodness of fit", the correlation coefficient, r , by $r = a_1 \frac{S_{\ln z}}{S_U}$

where $S_{\ln z}$ and S_U are the standard derivations of the height and velocity respectively

or $$r = \frac{n \Sigma U (\ln z) - \Sigma U \Sigma \ln z}{[n \Sigma (\ln z)^2 - (\Sigma \ln z)^2]^{1/2} [n \Sigma U^2 - (\Sigma U)^2]^{1/2}}$$

a_0 is the logarithm of the height at which the velocity, U , equals zero. In this case this height is better known as the roughness length, z_0 .

In actual practice the computer program that was designed to process data tapes for mean wind profile information had three basic functions. First the program counted the pulses for any desired time

interval and any given number of anemometers; secondly it converted the pulse count to velocities using the calibration curve for each anemometer; and thirdly computed the logarithmic curve fit for the data.

The Monin-Obukhov "similarity theory" states that near the surface a velocity u^*, a length L, and a temperature T* exist which are constant with height within the boundary layer. The length scale, L, is defined by Lumley and Panofsky (1964) as $L = -\frac{u^{*3} C_p \rho T}{K g H}$

where K is the von Karman constant; H is the vertical heat flux; and C_p is the specific heat at constant pressure. For near neutral stability conditions L approaches infinity since H approaches zero, thus the only meaningful length scale remaining is height. Therefore, based on similarity grounds, the differential equation for the wind profile is

$$\frac{\partial U}{\partial z} = \frac{u^*}{K z}$$

In its integrated form it becomes $U = \frac{u^*}{K} \ln \frac{z}{z_o}$

after applying the boundary condition $U = 0$ at $z = z_o$.

Having determined z_o by the curve fitting process, u^*, the friction velocity, can be determined for each wind profile. The importance of the friction velocity may be seen in the definition for given by Lumley and Panofsky (1964), $u^* = [\tau/\rho]^{1/2}$.

Vertical temperature gradients measured either visually by thermometers or recorded as thermister output and averaged over a ten minute sampling period should that over 98% of the profiles could be considered to possess near neutral stability (Richardson number $R_i \leq 0.03$).

Therefore, assumptions required for the validity of a logarithmic wind profile appear to be justified.

Verification of Ruggles' (1969) results was attempted by processing 143 ten-minute mean wind velocity profiles; 94% of the profiles were found to have a correlation coefficient of 0.90 or greater, which compares with 96% for Ruggles data. This decrease can be partially explained by the orientation of the buoy and anemometers during a few data sampling periods. Buoy orientation was dependent upon the direction of the tidal current; therefore, it was possible for the cup anemometers to be sheltered by the instrument platform during two brief periods each day.

Figure 4 shows a plot of roughness length vs. the wind speed at ten meters averaged over ten minutes. Since data were gathered at different sites during different years, utilizing different anemometers and new computer programs, the results must be considered independent. Therefore his unusual results can be corroborated.

To futher investigate the possible causes of peaks in the roughness length at 2, 4 and 8 meters, a series of histograms were constructed. These histograms, displayed as figures 5 and 6, show the distribution of roughness length for 10 meter mean wind speeds of 700 to 810 cm/sec using 10cm/sec wind speed intervals . Their tendency toward a bi-modal distribution of roughness length will be discussed fully when the distribution of friction velocity and Reynolds stress is considered.

While valuable insights into the structure of the atmospheric boundary layer have been gained by the study of ten minute profiles, one

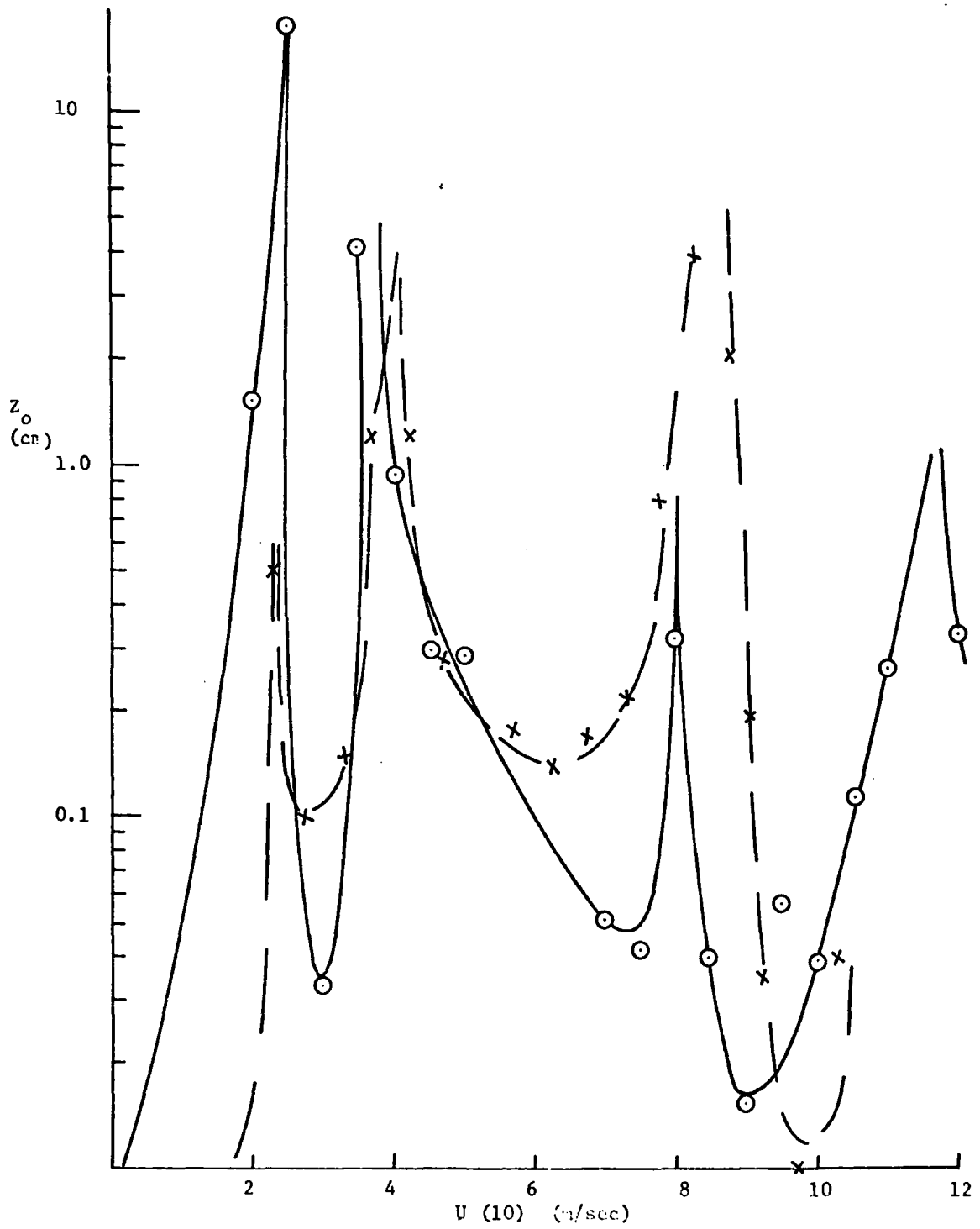

Figure 4: Roughness length as a function of 10 meter wind speed
⊙ CROSBY; x Ruggles (1966)

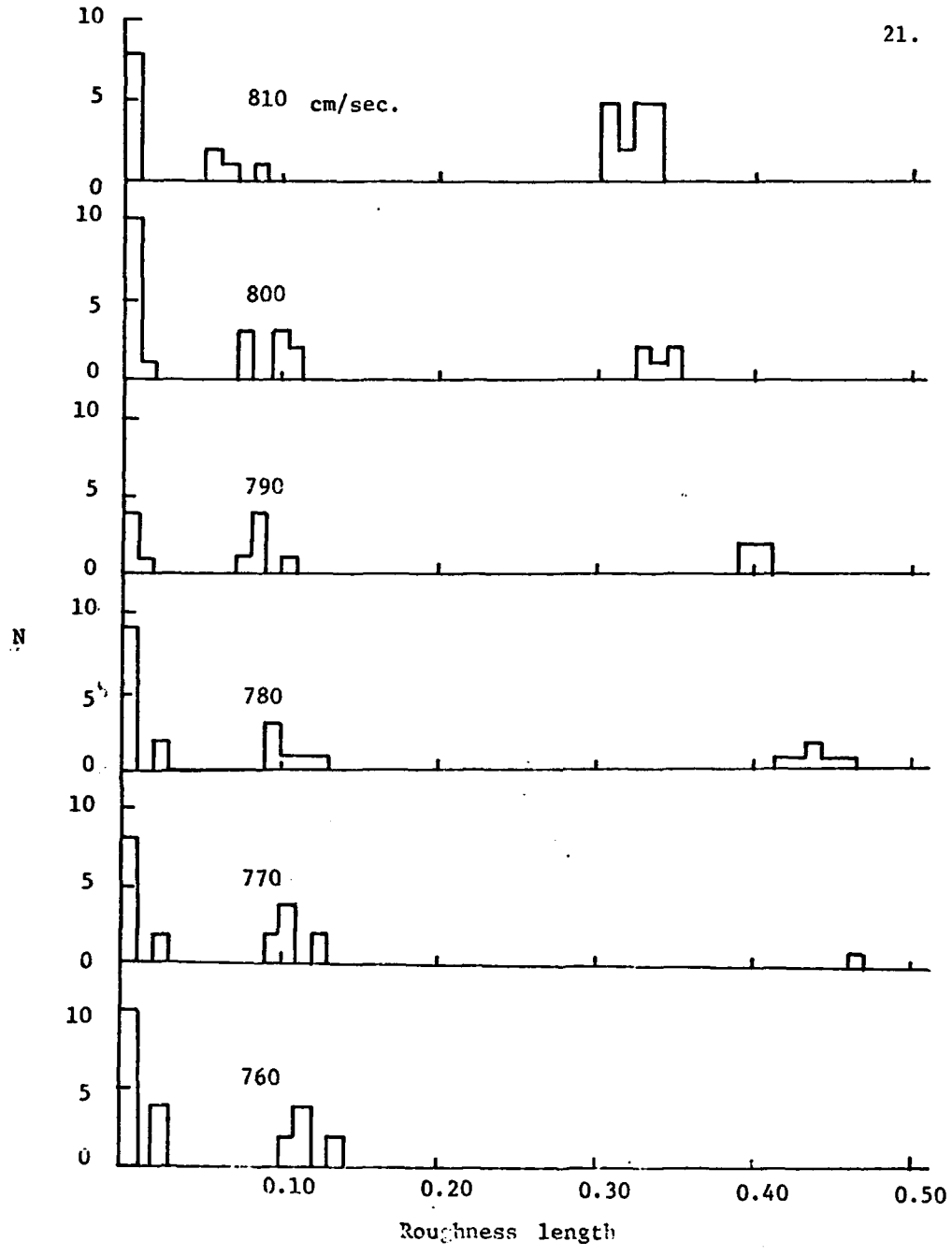

Figure 6: Roughness length distribution for U (10) = 760 to 810 cm/sec.

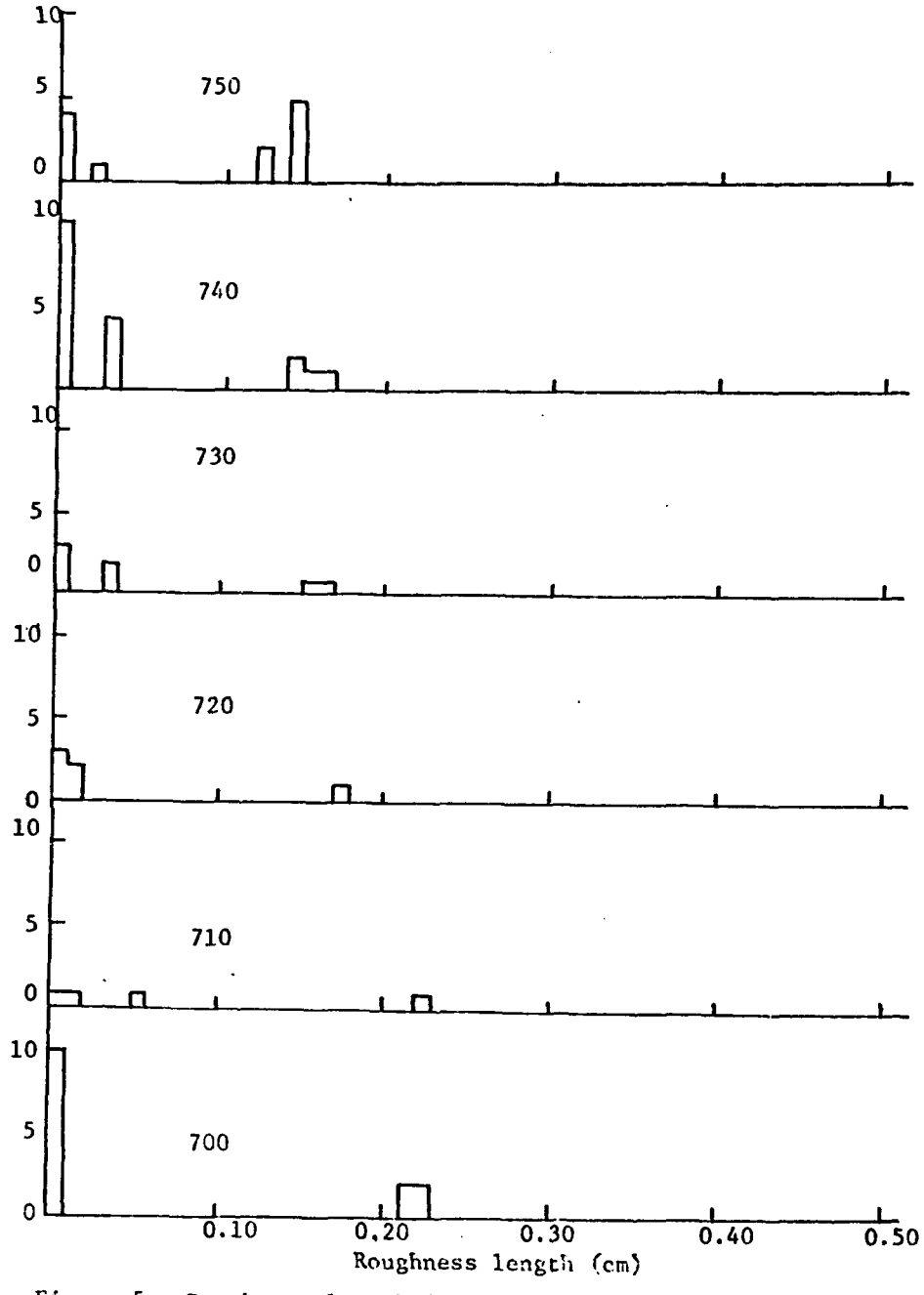

Figure 5: Roughness length distribution for U (10) = 700 to 750 cm/sec.

may ask the question; "How meaningful are the averaged results in the light of the known intermittent nature of the air flow?"

In order to determine the effects of intermittency on the mean wind profile an extensive analysis was made of the data recorded during runs 145 to 164. Since turbulence and hence intermittency is enhanced during periods when the lapse rate is unstable, these mean profile runs were chosen because they offered the greatest possibility of high Richardson numbers (cool air flowing over warm water during early fall).

Twenty, 10 minute average wind profiles were constructed from the data; the correlation coefficient for each run had a value of .98 or greater. Table 1 gives the observed 10 minute wind profile for each run and the resultant logarithmic fit correlation coefficient. To determine the important time scales of the intermittent events responsible for distorting the wind profile to an extent that it can no longer be considered logarithmic, the data for each run was analyzed using decreasing averaging periods until a significant decrease in the correlation coefficient was noted. Table 2 displays the data for run 160 which was chosen as representative of the series. Averaging periods were 10 minutes, 5 minutes, 1 minute, 30 seconds, 20 seconds and 10 seconds.

Run Number	Velocity 11.4m	7.5m	5.0m	3.7m	2.4m	Correlation Coefficient
145	906	864	812	763	732	0.99
146	848	813	770	728	703	0.99
147	855	817	769	723	699	0.99
148	860	830	788	747	722	0.99
149	941	904	869	833	807	1.00
150	998	969	942	919	882	1.00
151	843	810	787	772	737	1.00
152	851	825	807	796	764	0.99
153	964	932	912	895	858	1.00
154	994	952	909	876	846	1.00
155	977	934	890	845	815	1.00
156	1020	990	919	864	831	0.99
157	1075	1024	971	911	881	0.99
158	1202	1147	1089	1022	981	0.99
159	1242	1188	1113	1046	1004	0.99
160	789	767	755	748	716	0.98
161	1074	1024	972	911	881	0.99
162	670	632	606	582	562	0.99
163	794	753	708	670	637	0.99
164	840	805	773	741	711	1.00

Table 1: 10-minute wind profile and correlation with logarithmic curve (velocities in cm/sec.)

Averaging duration	Correlation coefficient					
10 minutes	0.98					
5 minutes	0.97	0.99				
1 minute	0.99	0.92	0.96	0.99	0.73	
	0.99	0.95	1.00	0.87	0.99	
30 seconds	0.97	1.00	0.96	0.86	1.00	0.87
	0.99	0.98	0.93	0.23	0.95	1.00
	1.00	0.82	0.99	0.99	0.87	0.86
	0.92	0.99				
20 seconds	0.96	0.98	1.00	0.54	0.97	0.86
	0.97	0.98	0.94	0.99	0.98	0.98
	0.96	0.24	0.27	0.85	0.98	0.97
	0.98	0.97	0.83	0.99	0.99	0.99
	0.97	0.55	0.69	0.97	0.97	0.99
10 seconds	0.84	0.93	0.88	0.98	0.96	0.86
	0.02	0.95	0.97	0.85	0.96	0.00
	0.90	1.00	1.00	0.39	0.00	1.00
	0.98	0.98	1.00	0.84	0.97	0.35
	0.99	0.71	0.43	0.12	0.24	0.31
	0.72	0.87	0.98	0.92	0.96	0.95
	0.97	0.98	0.94	0.76	0.33	0.95
	0.90	0.99	0.94	0.99	0.94	0.99
	0.97	0.93	0.00	0.87	0.31	0.84
	1.00	0.82	0.39	0.97	0.94	1.00

Table 2: Correlation coefficients for logarithmic profile fit for run 160 grouped by averaging time.

It is interesting to note that two profiles with a poor fit often combine in a longer averaging period to form a profile which is much more logarithmic in form. Looking at the first minute of run 160, for example, shows that 2 -10second profiles with correlation coefficients of 0.84 and 0.93, when combined, form a 20 second profile with a correlation coefficient of 0.96; similarly the next two, with values of 0.88 and 0.98, combined, have a correlation coefficient of 0.98 and the last two, with values of 0.96 and 0.86, combine to form a profile possessing a correlation coefficient of 1.00. This result is typical of all profiles analyzed in this manner; it is an indication that wind profiles tend toward a logarithmic form for longer averaging periods. Figure 7 indicates the probability of occurance of a logarithmic profile (a correlation coefficient of 0.95 or greater) as a function of averaging period for moderate or higher wind speeds. For light wind speeds a "least count" situation may occur since one pulse count can be 10-20% of the total count for short averaging durations at low wind speeds.

Figure 8 shows the variation of correlation coefficient verses time for the logarithmic wind profile obtained using 10, 20 and 30 second averaging periods. As may be noted from Table 2, one minute average wind profiles had a correlation of less than 0.95 only during minute 2, 5 and 9, while there are disturbed profiles during 8 of the ten minute periods when one considers features of a small time scale (10 second average wind profiles). Figure 9 shows an isotach analysis of the 10 second average profiles for run 160. Characterizing each case of a distorted profile is an inflection point in the velocity profile; that

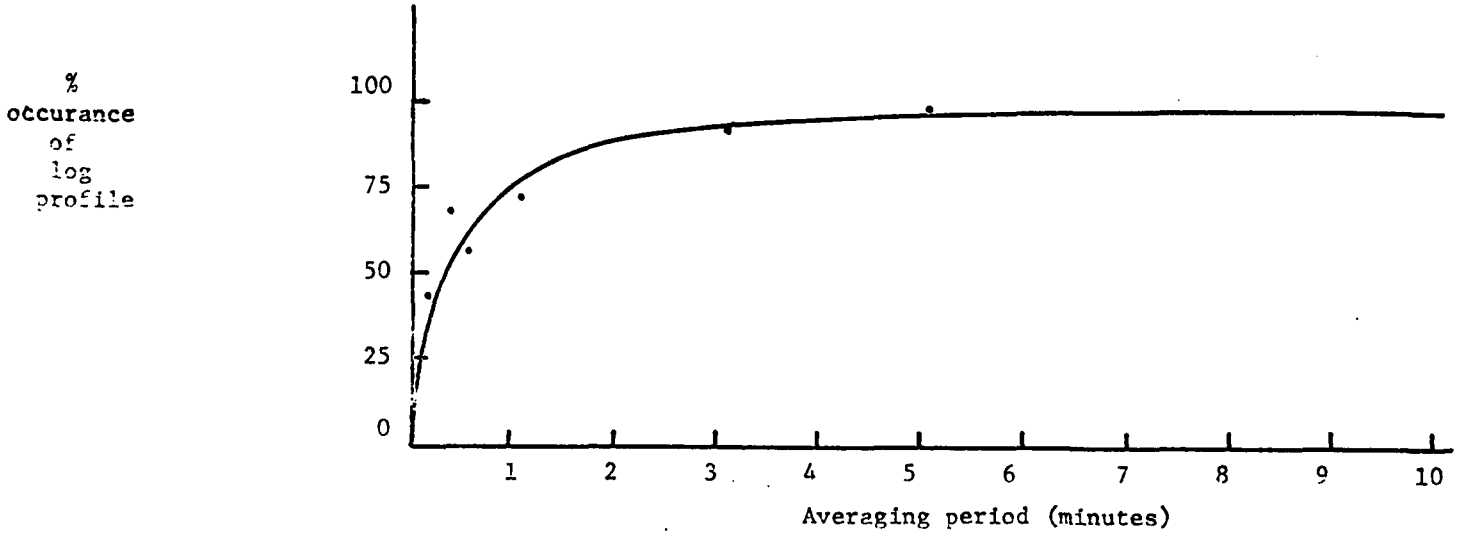

Figure 7: Percent occurance of logarithmic profile (r ≥ 0.95) as a function of length of averaging interval. Run 145 to 164. observed for run 160.

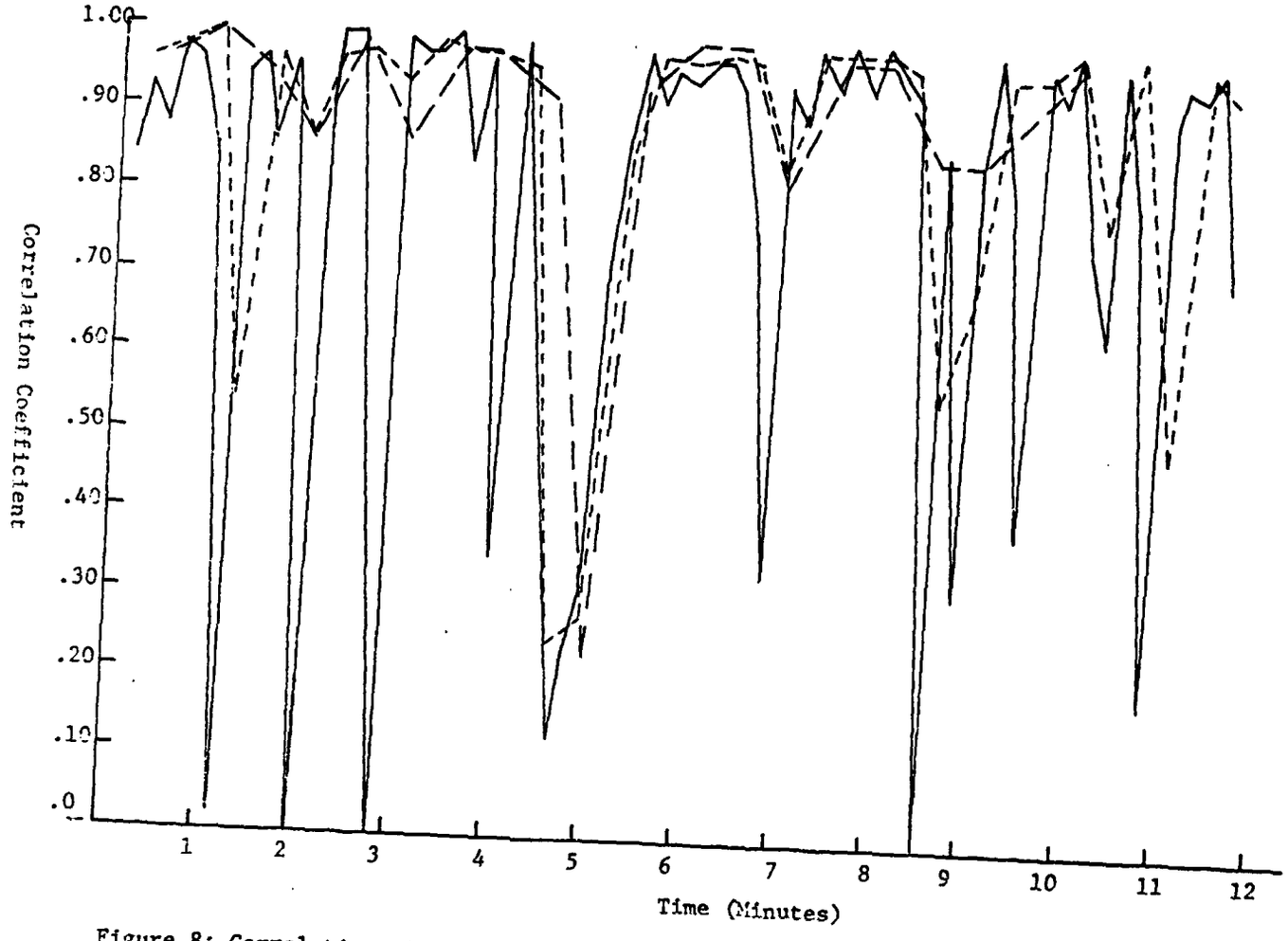

Figure 8: Correlation with logarithmic curve vs. time for run 160.

———— 10 second, - - - - - - - 20 second, — — — — 30 second average profile.

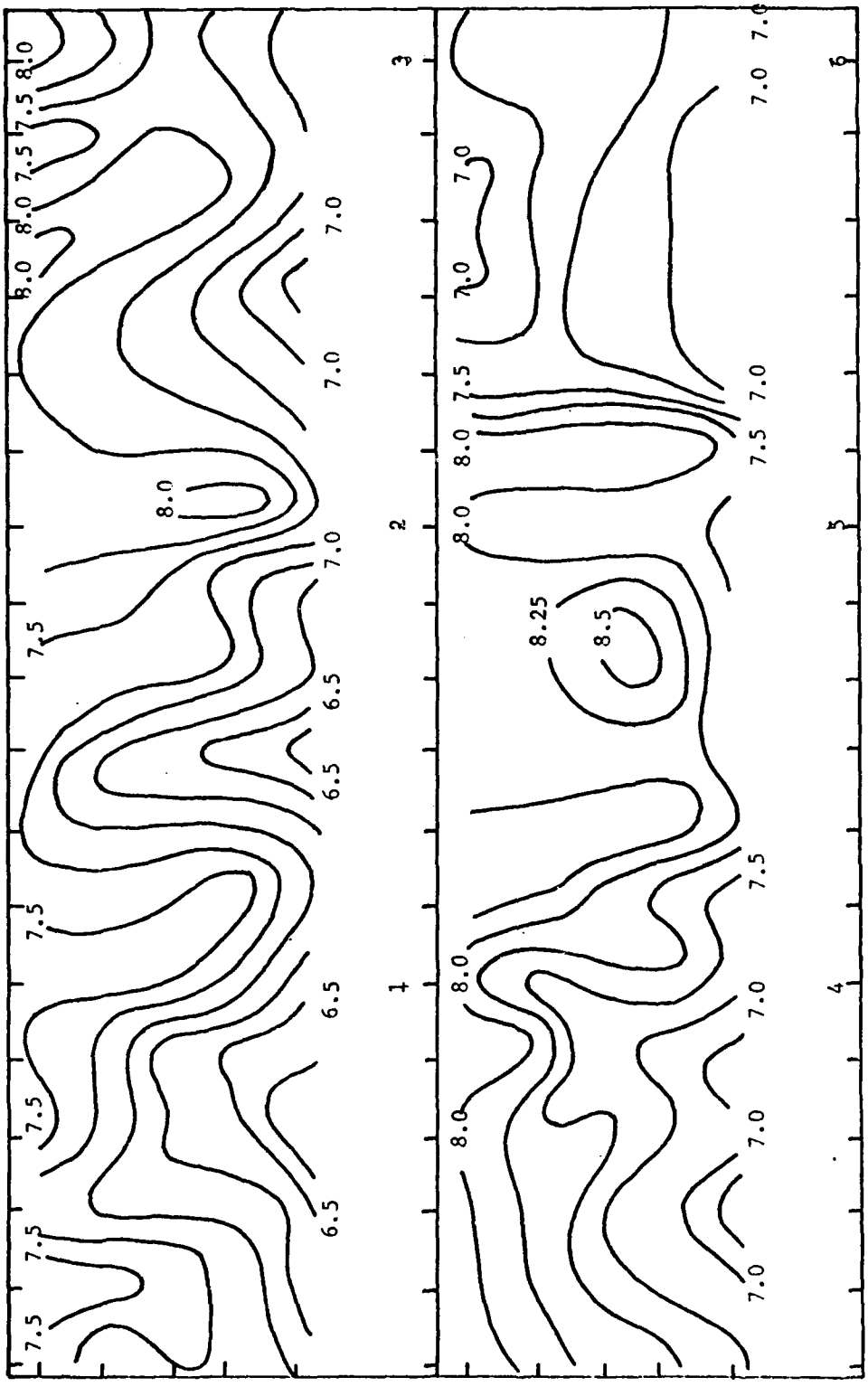

Figure 9: Isotach analysis for run 160, Velocities in m/sec.

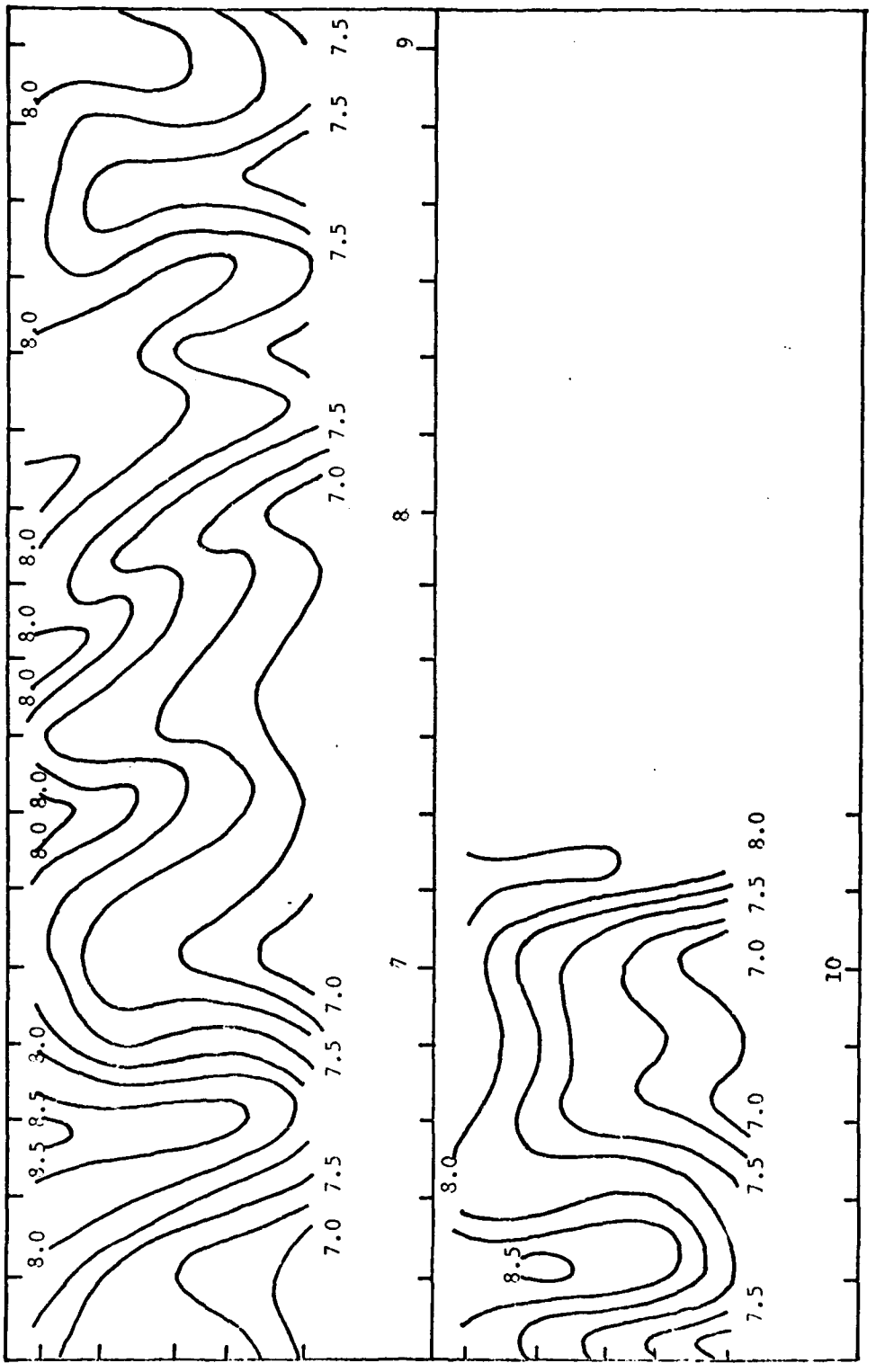

Figure 9: (Cont'd).

is there is a point in the profile where $\frac{\partial U}{\partial z} = 0$. The inflection points in the velocity profile are readily apparent in the plots of the 10 second wind speed profile (Figure 10).In these plots the wind speeds of each of the 10 second profiles are adjusted such that

$$U(10) = \bar{U}(10)$$

where $\bar{U}$ is defined as a 1 minute average profile). Since the shear of the mean wind profile is important in the determination of the turbulent energy production one can logically look at the effects of small time scale features on the turbulent energy equation.

In order to investigate the production of turbulent energy, the Boussinesq form of the momentum equation is written in the form of mean and fluctuating components. That is

$$\vec{u} = \vec{U} + \vec{u}'$$

$$p = P + p'$$

$$\vec{b} = \vec{B} + \vec{b}' \qquad \text{where} \qquad \vec{b} = -\vec{g}\frac{\rho - \rho_0}{\rho_0}$$

Thus $$\frac{\partial}{\partial t}(U+u')_i + (U+u')_j \frac{\partial}{\partial x_j}(U+u')_i + \varepsilon_{ijk}\Omega_j (U+u')_k$$

$$+ \frac{1}{\rho_0}\frac{\partial}{\partial x_i}(P+p') + (B+b')\delta_{i3} = \nu \frac{\partial}{\partial x_j}\frac{\partial}{\partial x_j}(U+u')_i$$

where ε_{ijk} $= 1$ for cyclic permutation of the 3 indicies

$= -1$ for anticyclic permutation

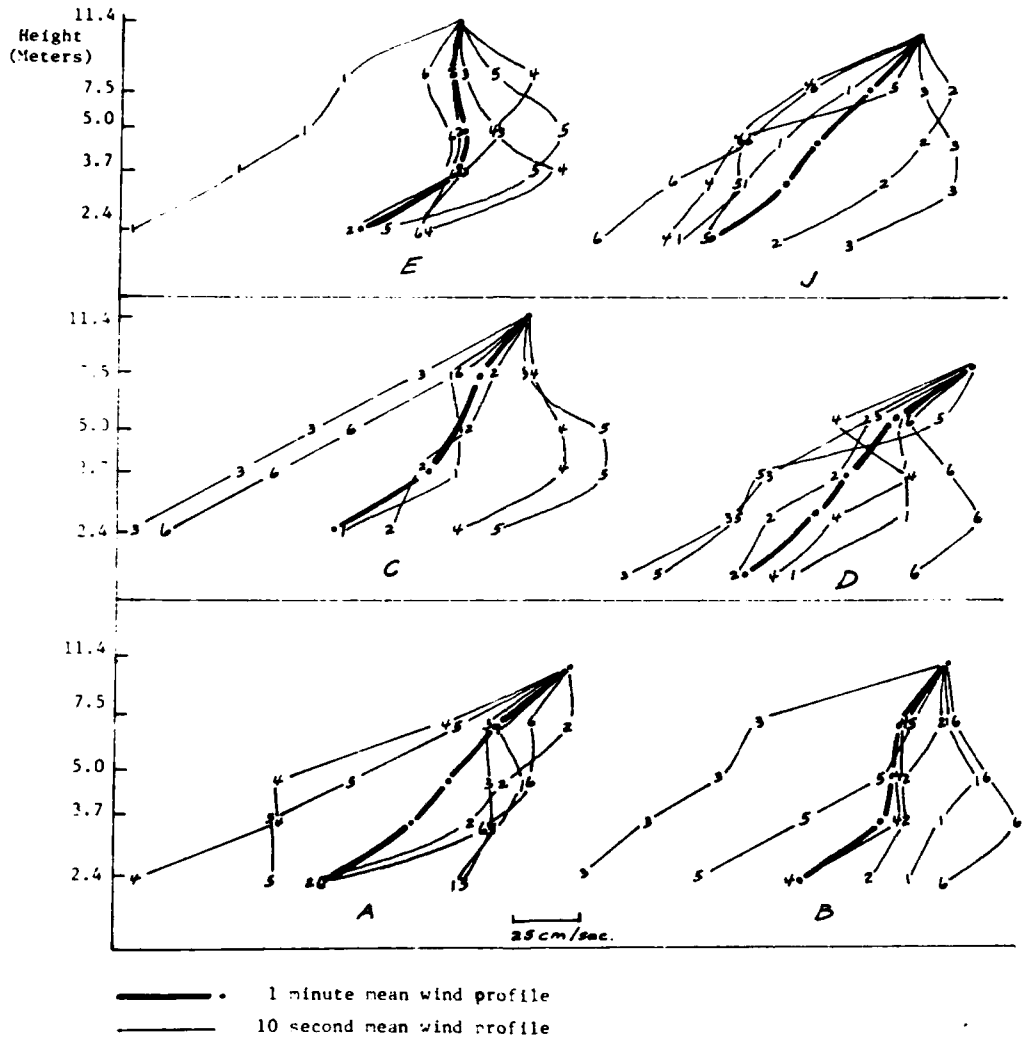

Figure 10: Wind speed profiles for run 160.

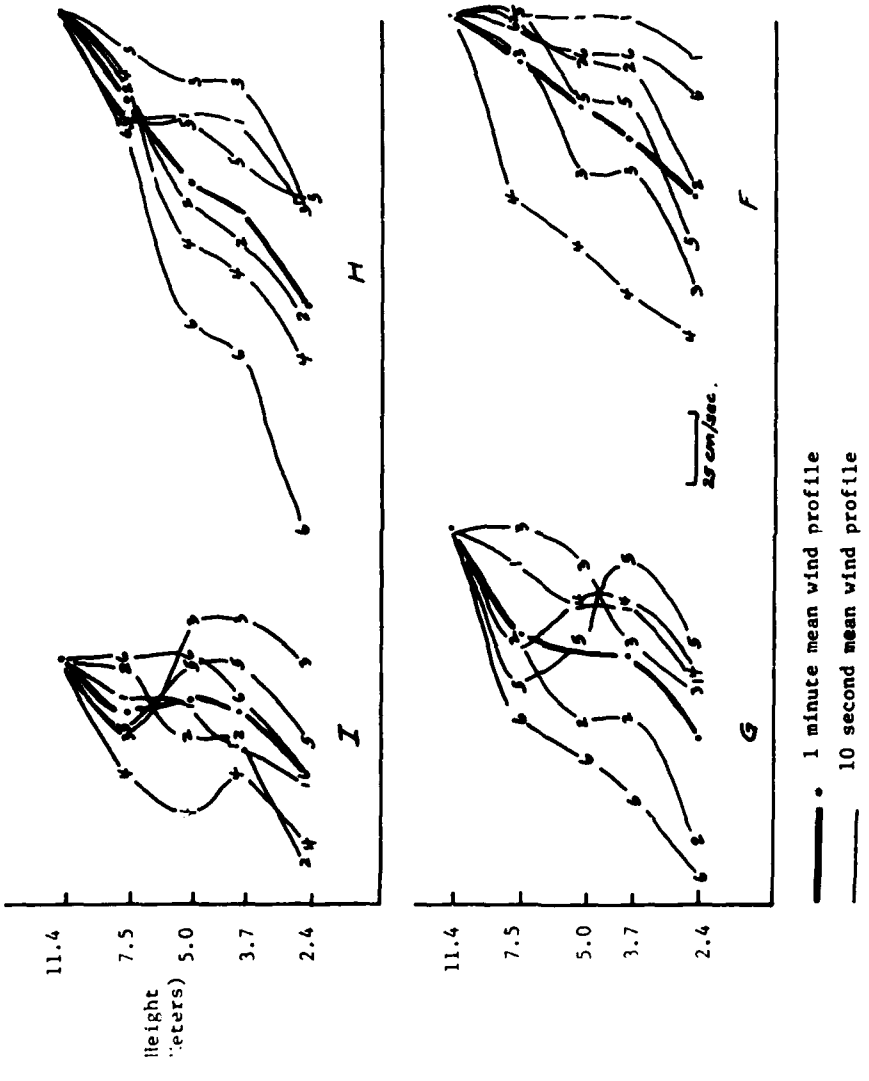

Figure 10: (cont'd)

Taking the scalar product of this equation and the fluctuating velocity component and then averaging the resulting equation yields

$$\overline{u_i' \frac{\partial u_i}{\partial t}} + \overline{u_i u_j' \frac{\partial}{\partial x_j} U_i} + \overline{u_i' u_j' \frac{\partial}{\partial x_j} u_i'} + \overline{u_i' U_j \frac{\partial}{\partial x_j} u_i'}$$

$$+ \overline{u_i' \varepsilon_{i3k} \Omega_3 u_k'} + \overline{\frac{u_i'}{\rho_0} \frac{\partial P}{\partial x_i}} - \overline{u_3' b'} = \nu \overline{u_i' \frac{\partial}{\partial x_j} \frac{\partial}{\partial x_j} u_i'}$$

since $\overline{(\bar{a})} = \overline{A + a'} = \bar{A} + \overline{a'} = A$

combining terms and envoking the continuity equation ; $\frac{\partial u_j}{\partial x_j} = 0$,

gives

$$\left(\frac{\partial}{\partial t} + U_j \frac{\partial}{\partial x_j}\right) \overline{\frac{u_i'^2}{2}} + \frac{\partial}{\partial x_j}\left[u_j' \left(\frac{p}{\rho_0} + \overline{\frac{u_i'^2}{2}}\right)\right] = -\overline{u_i' u_j'} \frac{\partial U_i}{\partial x_j} + \overline{w' b'} - \epsilon$$

where ϵ is the rate of energy dissipation by molecular viscosity. Thus the rate of change of the turbulent kinetic energy + the divergence of energy flux = the rate of transfer from the mean flow by the working of the Reynold stresses against the velocity gradient (the production term) + the vertical buoyancy flux + the rate of dissipation. In this study the flux term will be neglected since it only serves to redistribute energy already present.

Since the mean flow is quasi-horizontal and the turbulence is approximately homogenous in the horizontal and by selecting cases where buoyancy effects are unimportant (near neutral stability), the turbulent energy equation may be simplified to $\frac{\partial}{\partial t} \overline{\frac{u'^2}{2}} = -\overline{uw} \frac{\partial U}{\partial z} - \epsilon$.

The friction velocity is defined as $u^{*2} = \overline{uw}$. The differential form of the equation for the logarithmic form of the wind speed profile is $\frac{\partial U}{\partial z} = \frac{u^*}{kz}$. Thus the production term can be evaluated from a profile analysis since, by making the indicated substitutions; $\overline{uw}\,\frac{\partial U}{\partial z} = \frac{u^{*3}}{kz}$

Figure 11 shows a plot of the production term as determined from wind profile analysis of both the 10 second and 1 minute averaged profiles. Probably the most striking feature of this figure is the large variability of the production term, but the most significant feature is the large value of the production term found by analyzing 10 second average profiles when compared to that of 1 minute averaged profile values. The one minute averaged profile production term varies between 12 and 441 cm^2/sec^3 while the ten second averaged profile production term values range between -2 and 2428 cm^2/sec^3 clearly demonstrating a fallacy in wave generation theories which assume the atmosphere to be an infinite, uniform source of energy and also shows the importance of efforts directed toward the explanation of wave generation by intermittent events. Surely when the turbulent energy production can be shown to vary by an order of magnitude of 10^3 over time intervals of the order of ocean surface wave periods this must be considered significant.

Calculation of the root mean square deviation for the production term yields a value of 491 cm^2/sec^3, while the average production is 296 cm^2/sec^3. By arbitrarily defining intermittency as turbulent production

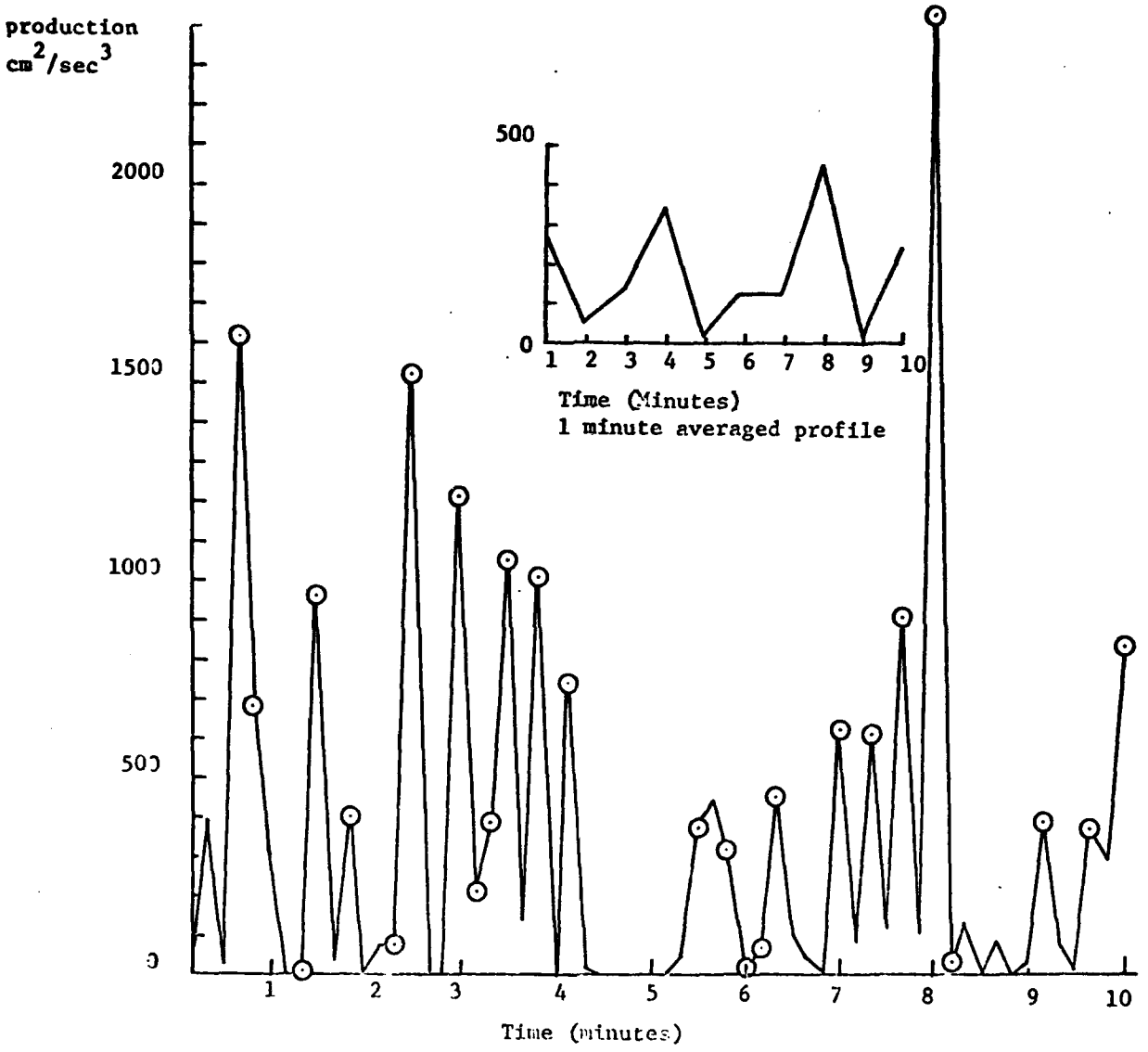

Figure 11: Turbulent energy production vs. time from 10 second averaged profile. Run 160 ⊙ profile values where r ≥ 0.95.

greater than two root mean square deviations from the 10 minute mean wind profile value (176 cm^2/sec^3), figure 11 shows that run number 160 was 8.3% intermittent. Thus it becomes obvious that the lower portion of the maritime atmosphere may be best described as a turbulent fluid whose turbulent energy production varies by three orders of magnitude in time scales of the order of ocean surface wave periods, and that these high turbulent energy production events occur approximately 10% of the time for moderate wind speeds.

A qualitative description of the sequence of events in the lower atmosphere may be obtained by use of Figures 8, 9, 10 and 11. While the proper starting point for this discription is questionable, the sequence is relatively easy to follow. To start, the profile eventually assumes a large stress, large shear form (see profile 6, figure 10-H). This yields a high rate of turbulent energy production; it also produces the upper peak on the roughness length histogram (figures 5 and 6). Not being an unbounded energy source, the atmosphere's support of this production is limited and the production is turned off by the injection of high velocity air into the lower portion of the profile. The profile, now having an inflection point which moves toward the ocean surface as time advances, becomes highly distorted and non-logarithmic. Comparison of figures 8 and 11 show that the most distorted profile (r = minimum) occurs approximately 20 seconds after the production term has reached its maximum value. It is difficult to determine how this higher velocity air is distributed in the lower portions of the profile but it is obvious that the profile shape rapidly returns to a more logarithmic

form.

It would be extremely difficult to model a regime such as that described above, but the effects of this variability are significant and must be considered in future wind wave generation theories.

In addition to gaining insight into the small scale nature of the atmospheric boundary layer, this investigation has shown the high probability of occurance of a logarithmic wind profile ($r \geq 0.95$) for long averaging periods. This knowledge of a long term mean logarithmic wind profile is extremely important to the field investigator in that it provides him with both a means of conducting in-situ calibrations and also a method of checking the individual anemometers for reliability. If, for example, the cups of an anemometer were distorted by an exceptionally high wave or by a bird flying into the cups, this situation could be discovered immediately even if the data were being recorded remotely, by analyzing the wind profile averaged over 30 minutes and noting the deviation of one anemometer from the others. When the damaged set of cups have been replaced an on site calibration can be conducted by comparison of the repaired anemometer's counts per 30 minutes to the best fit logarithmic profile of the previously calibrated anemometers. Without assuming a logarithmic profile the anemometer would have to be removed, calibrated, and replaced.

Proper performance of equipment in the field may also be tested. Mollo-Christensen (1968) analyzed the distortion of the wind field due to the R/V FLIP superstructure by means of a series of wind tunnel experiments. In order to determine the effects of this unusually shaped instrument

platform in the open ocean, wind profile data obtained during BOMEX (Superior [1969]) were analyzed for each of 6 days. The minimum averaging period was 6 hours. Figure 12 is a plot of the averaged wind profiles; it also displays the shape of the R/V FLIP when the ship is in its vertical position. A correlation coefficient for the averaged wind profiles was 0.85. While the results of one case study can not be considered as conclusive, they do show that a complete investigation of possible distortion to the wind profile is required before extensive analysis of the profile determined Reynolds stress, or in fact any profile parameters, may be undertaken.

Yet another use of the high probability of a logarithmic profile may be found.

If one is interested in the average friction velocity or roughness length for periods of 10 minutes or longer, computation may be reduced by assuming the profile to be logarithmic (Figure 7 shows this is a valid assumption 95% of the time). The profile parameters may be obtained as follows: using figure 13 and the wind speed shear computed between two levels obtain the friction velocity, next enter figure 14 with the friction velocity and the ten meter wind speed to obtain the roughness length. This method requires only two data channels for anemometry and no computation to yield the required profile parameters.

The bi-modal distribution of roughness length discussed earlier in the above chapter remains to be explained. Since the logarithm of roughness length is proportional to the friction velocity, and since friction velocity or stress is intuitively more meaningful, the friction velocity

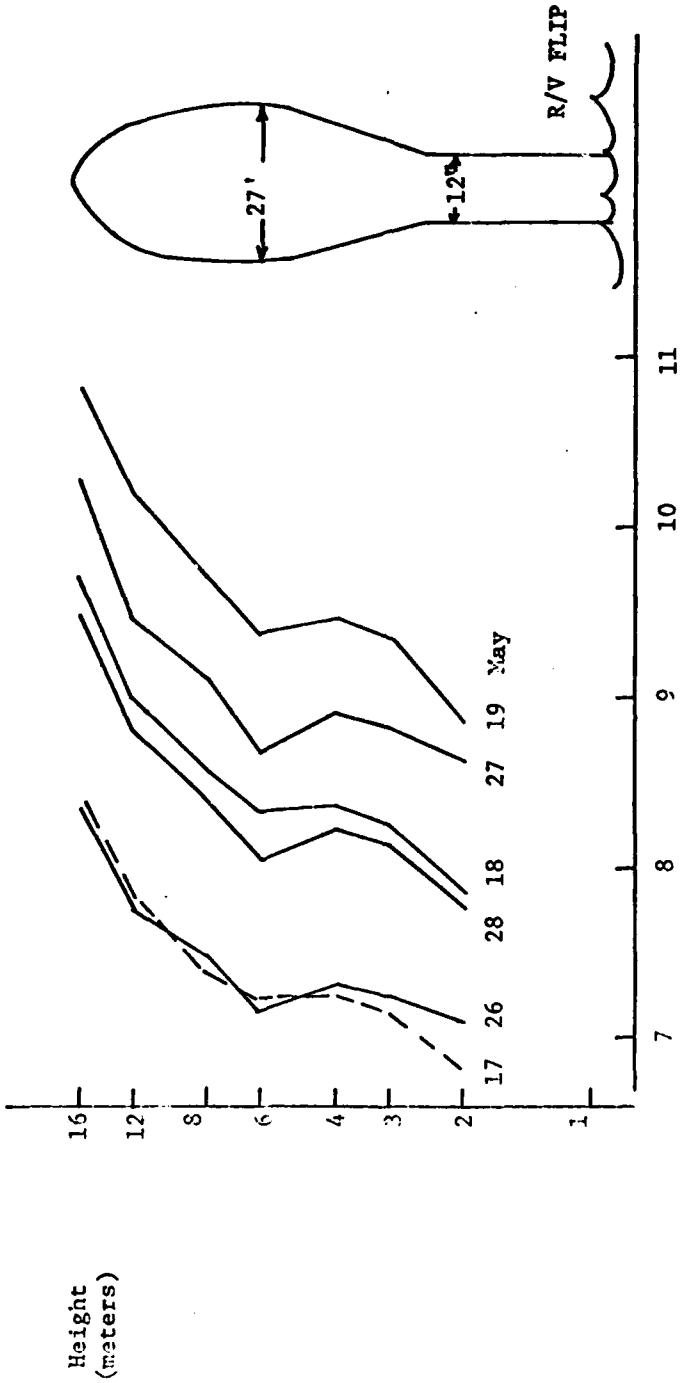

Figure 12: Averaged daily wind speed profiles from R/V FLIP.

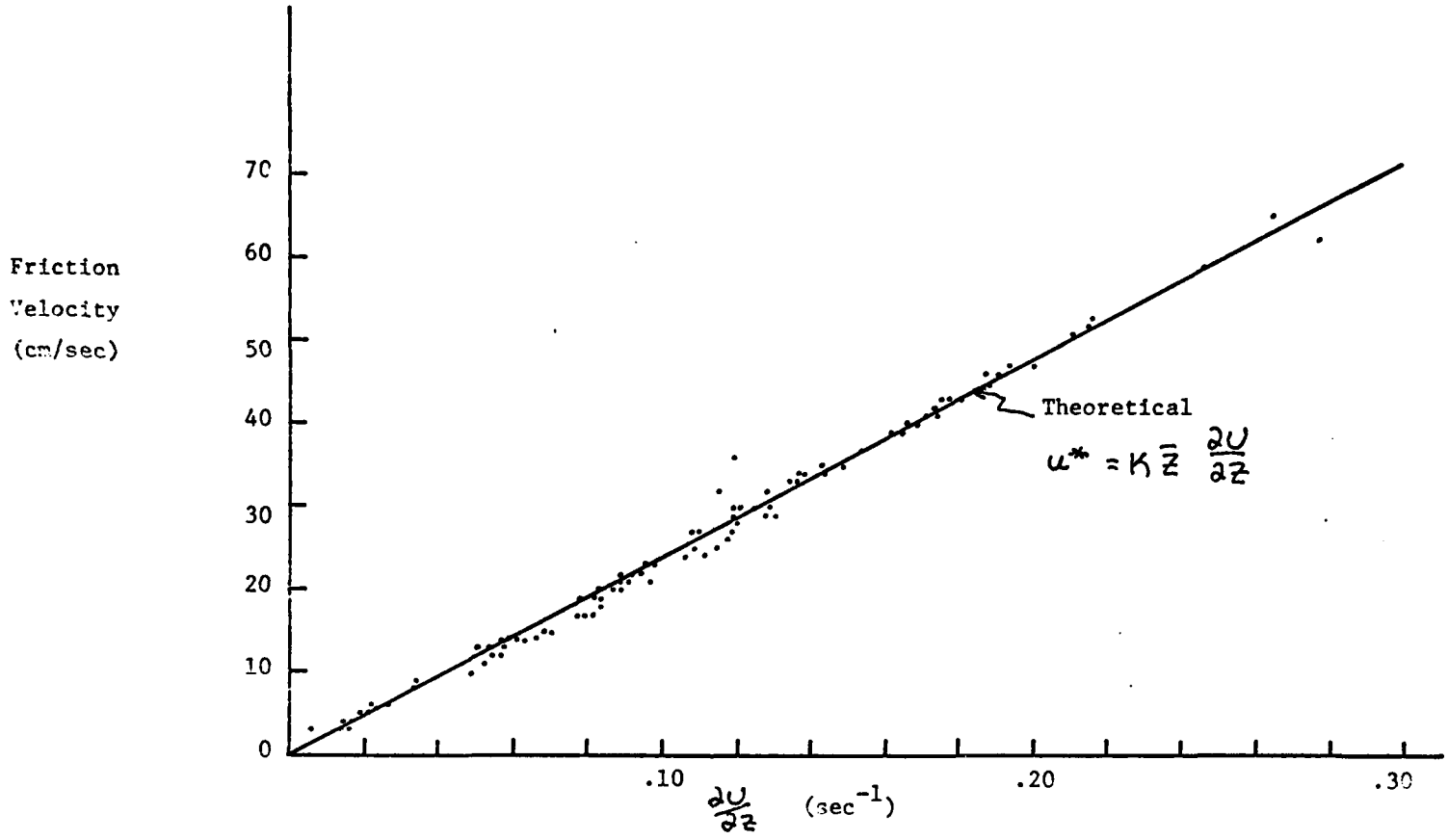

Figure 13: Friction velocity as a function of wind speed shear • observed for runs 70 to 178.

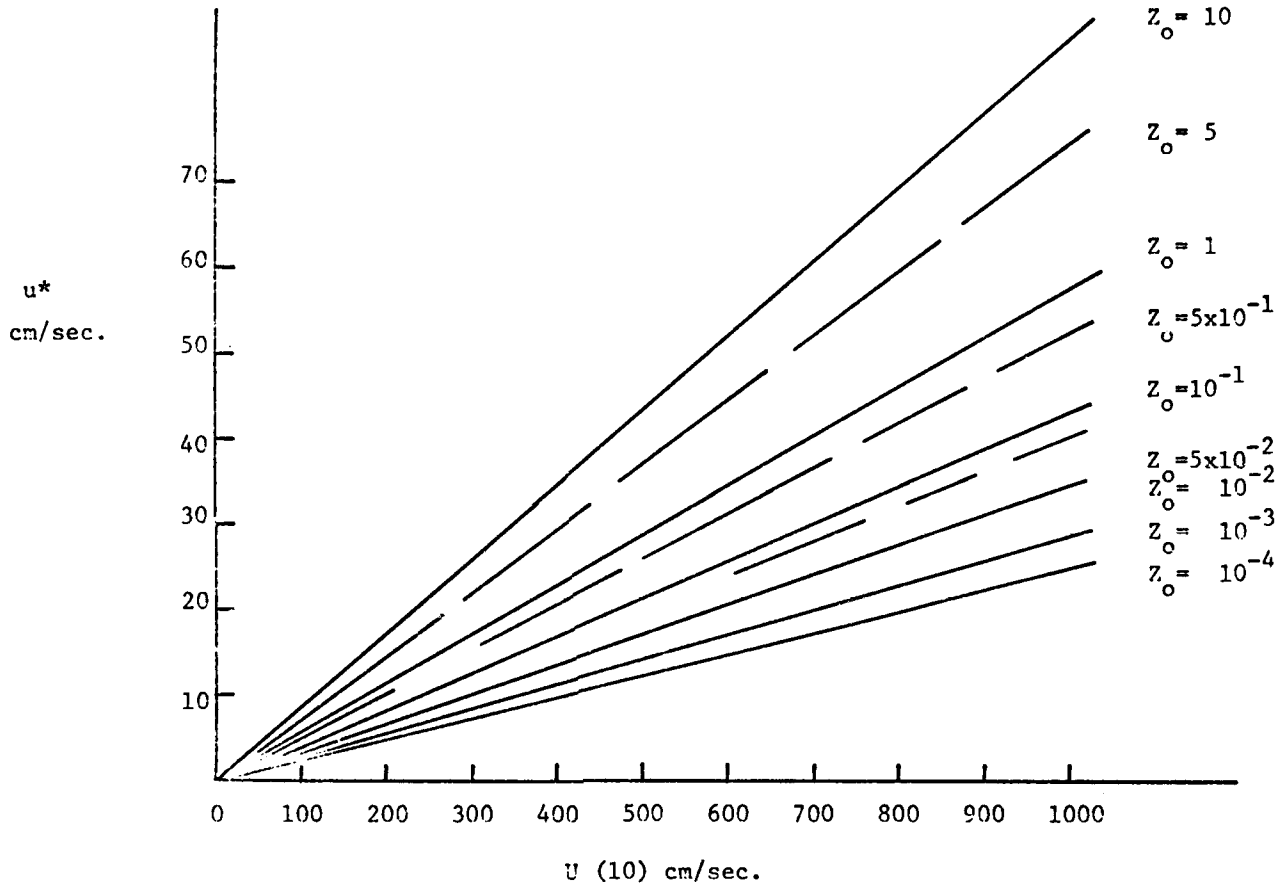

Figure 14: Roughness length as a function of u* and 10 meter wind speed.

distribution was analyzed in detail Figures 15 A & B show a plot of the distribution of friction velocity as a function of the ten meter wind speed. It becomes immediately obvious that the linear relationship,

$$u^* = 0.04\ U(10)$$

reported by Ruggles (1969) does not exist in this study. These diagrams display the bi-modal distribution of friction velocity in the vicinity of 4 and 8 m/sec and the uni-modal structure between. This again supports the visually observed Beaufort scale class boundaries (for fuller discussion see Ruggles [1969]). These figures show that, at the class boundaries of 4 and 8 m/sec, the wind field may exhibit the stresses of either the wind speed region directly above or directly below the boundary. Thus the Reynolds stress at 8 m/sec may be similar to that of 9 m/sec at one instant and to that of 7 m/ sec at the next moment. It may also be noted that there appears to be a linear relationship between friction velocity and the ten meter wind speed within class boundaries.

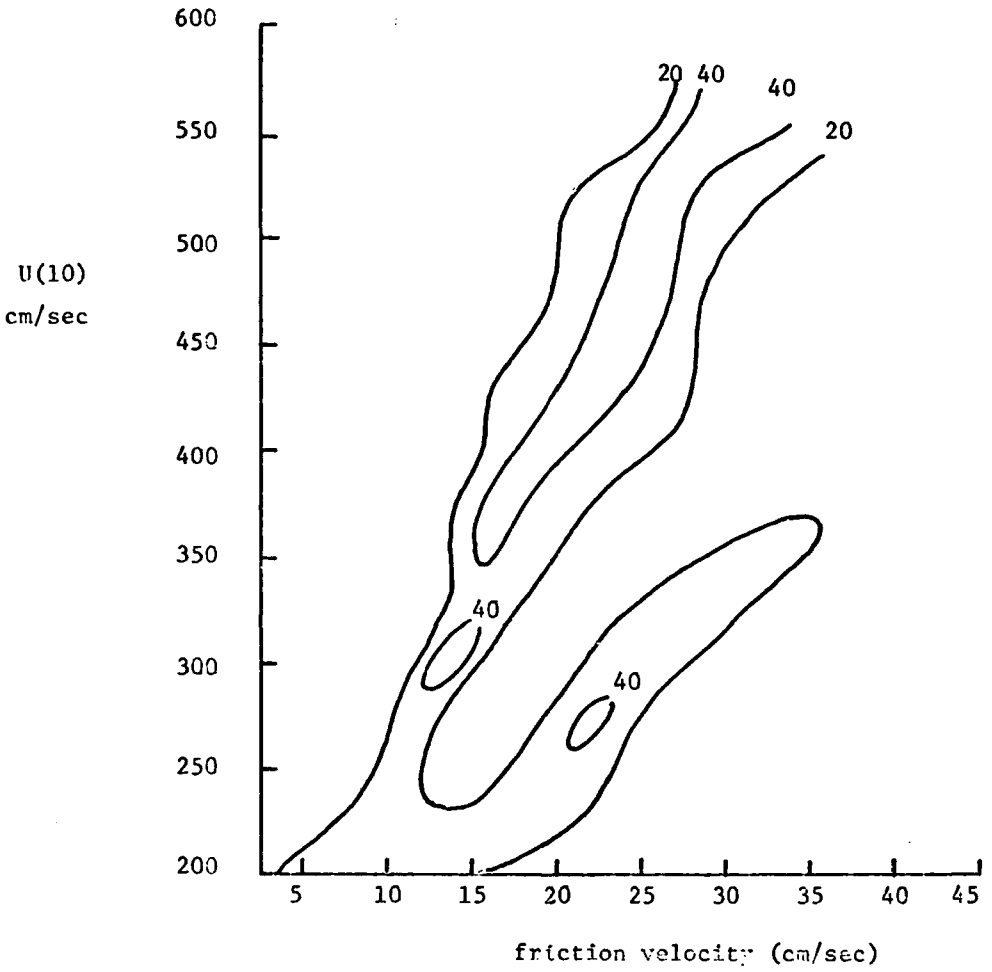

Figure 15A: A distribution of friction velocity as a function of the 10 meter wind speed. Contours in percent.

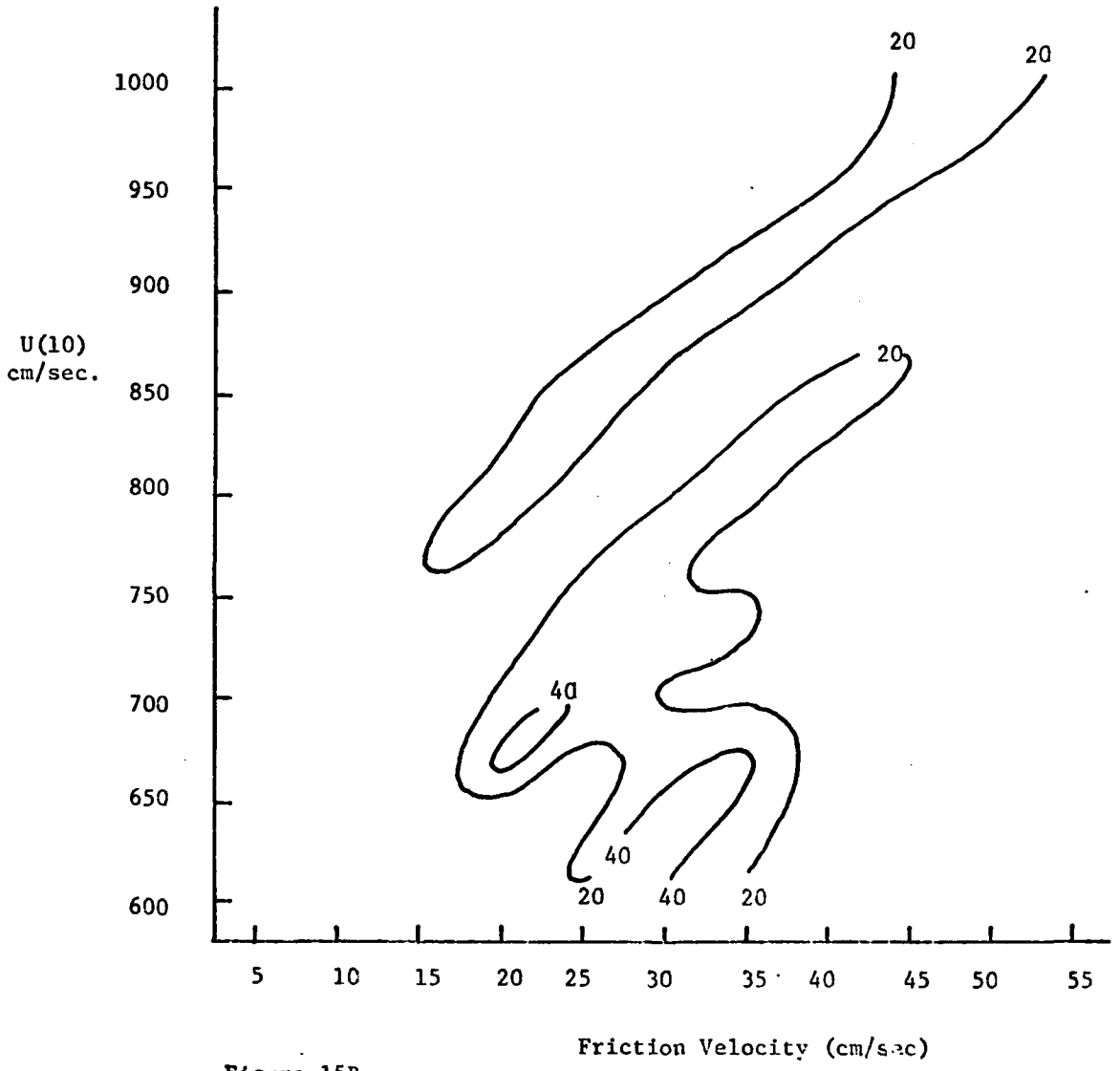
20
20
20
40
40
20
40
20
1000
950
900
850
800
750
700
650
600
U(10)
cm/sec.
5
10
15
20
25
30
35
40
45
50
55
Friction Velocity (cm/sec)

Figure 15B

IV. Summary of Results and Recommendations

The results of this report confirm the findings of Ruggles (1969) regarding the logarithmic nature of the 10 minute mean wind speed profile over the open ocean with one notable exception. The linear relationship, $u^* = 0.04\ U(10)$, reported by him does not exist in the data analyzed in this study. Within boundaries defined by the singularities in the roughness length at 2, 4, 8 and 12 meters/second, a functional relationship between the wind speed at 10 meters and the friction velocity appears to be present. The singularities in the roughness length appear as a result of a transition between differing wind stress regimes. In these zones average roughness length is meaningless in that the mean is rarely occupied and its value is largely determined by the variability of the wind profile, that is the percent of the time a high stress, high roughness length situation occurs as against the time a low stress, low roughness length regime is present. For run 160, for example, the upper peak in the roughness length distribution was occupied 6.7% of the time. This compares favorably with the value of 8.3% obtained in Chapter III as a measure of the intermittency of the wind field during this run.

While intermittent "events" are shown to occur only 5 to 10% of the time when one uses the 95% significance level as a criteria, the magnitude of these events is extremely inportant if the turbulent energy of the atmosphere is considered. Turbulent energy production as determined from wind profile analysis varies by a factor of 10^3 over time intervals of the order of surface wave periods. A study, similar to the one conducted in Chapter III, should be undertaken to investigate the mean wind

speed profile over a non-undulating surface. It is important to differentiate between the characteristics of the wind profile attributable to the energy source/sink features of the underlying surface and those characteristics common to all turbulent wind fields.

An analysis of mean wind speed profiles, obtained under conditions of near-neutral stability, was undertaken using averaging periods of 10 seconds to 10 minutes. The results of this effort indicate that there is a trend toward a more logarithmic form of the mean wind profile as the averaging period is increased. For 10 minute average wind profiles, there is a 95% probability that the profile will be logarithmic ($r \geq 0.95$) while less than 50% of the profiles may be considered logarithmic when 10 second averages are considered. All field investigators utilizing a vertical array of anemometers are encouraged to use this observed profile form as a consistency check and periodic calibration check of their equipment. If long period average wind speeds show significant deviation from the expected logarithmic value, the data should immediately become suspect and further investigation of the instruments should be initiated. In this report the mean wind speed profiles obtained aboard the R/V FLIP were averaged over 1 day periods. These wind profiles had an average correlation coefficient of 0.85. The Reynolds stress and roughness length determined from the profiles must, therefore, be used with caution.

Finally, it was noted that if one is interested only in roughness length and friction velocity, averaged over 10 minutes or more, these parameters may be obtained expeditiously by using two anemometers and figures 13 and 14 of Chapter III.

Acknowledgements

The author wishes to thank Professor Erik L. Mollo-Christensen at the Massachusetts Institute of Technology for his support, advice, and counsel during the period of this investigation. His patience and encouragement during periods of dispair were most helpful.

Without the electronic expertise of Mr. Kenneth A. Morey and Mr. James H. Peers Jr this investigation would have been impossible. Their devotion to the project contributed immeasurably to the success of this study.

The help of Mr. Louis LeTourneau, Mr. Robert Paquette and Mr. Steven Ricci is very much appreciated. I will always be deeply indebted to Mrs. Heide Pickenhagen for typing of the manuscript.

Finally a special thank you to LCDR. Craig E. Dorman for his help both in the field and in the analysis phase of the project.

References

Lumley, J.L. and Panofsky, H.A., 1964, The Structure of Atmospheric Turbulence, John Wiley and Sons, New York.

Mollo-Christensen, E.L. and Dorman, C.E., 1971, A buoy system for air-sea interaction studies, M.I.T., Department of Meteorology, Technical Report.

Mollo-Christensen, E.L., 1968, Wind tunnel test of the superstructure of R/V FLIP for assessment of wind field distortion; M.I.T., Fluid Dynamic Laboratory, Technical Report.

Ruggles, K.W., 1969, Observations of the wind field in the first ten meters of the atmosphere above the ocean; M.I.T., Dept. of Meteorology, Technical Report.

Superior, W.J., 1969, Bomex flux and profile measurements from FLIP, C.W. Thornthwaite Associates Laboratory of Climatology, Technical Report.

Van Atta, C.W. and Chen, W.Y., 1970, Structure functions of turbulence in the atmospheric boundary layer over the ocean, J. Fluid Mech., 44, 145-159.

Warsh, K.L., Garstang, M. and Grose, P.L., 1970, A sea-air interaction deep-ocean buoy, J. Marine Res., 28, 99-111.